



Full Length Article

Anchoring metal-organic framework nanoparticles on graphitic carbon nitrides for solar-driven photocatalytic hydrogen evolution

Lin Tian^a, Xiaofei Yang^{a,b,c,*}, Qinqin Liu^a, Feiqiang Qu^a, Hua Tang^{a,*}

^a School of Materials Science & Engineering, Jiangsu University, Zhenjiang 212013, PR China

^b College of Science, Nanjing Forestry University, Nanjing 210037, PR China

^c State Key Laboratory of Photocatalysis on Energy and Environment, Fuzhou University, Fuzhou 350116, PR China



ARTICLE INFO

Keywords:

g-C₃N₄

MOF

ZIF-8

Photocatalytic hydrogen evolution

Water splitting

ABSTRACT

The development of low-cost and noble metal-free photocatalytic materials with precisely controlled morphologies and interfaces is vital to achieving highly efficient solar-to-fuel conversion. We herein report the fabrication of novel metal-organic framework (MOF)/g-C₃N₄ heterostructured materials with well-defined micro-/nanostructures and intimate interfacial contact. Zeolitic imidazolate framework-8 (ZIF-8) nanoparticles are found to be evenly anchored on modified rod-like g-C₃N₄ materials. The resultant hybrid materials demonstrate the integration of two components and show enhanced light-harvesting property in the visible light region. ZIF-8/g-C₃N₄ composite materials have been employed as the catalysts for solar-driven photocatalytic hydrogen evolution from water splitting. Under light emitting diode (LED) illumination, ZIF-8/g-C₃N₄ composite photocatalysts exhibit significant hydrogen-evolving performance in comparison to bulk ZIF-8 material. The enhanced hydrogen production efficiency can be ascribed to synergistic improvements in electron-hole separation, charge transportation and redox capability. This synthetic strategy can be extended to the design and controllable synthesis of a variety of MOF-based composite materials for energy and environmental applications.

1. Introduction

Inspired by natural photosynthesis, a variety of semiconductor-based catalysts with well-matched bandgap diagrams have been considered to be candidates for solar-driven photocatalytic water splitting over the past few decades [1–5]. Photocatalytic water splitting involves the two-electron hydrogen evolution reaction (HER) and four-electron oxygen evolution reaction (OER), representing one of the most promising ways to convert solar energy into clean and sustainable fuels [6–8]. Since the pioneering work of Fujishima and Honda on TiO₂ photoanode for water splitting, intensive efforts have been made to develop high-performance hydrogen-evolving photocatalysts for visible-light-driven water splitting [9–17]. Among them, polymeric graphitic carbon nitride (g-C₃N₄) reported by Wang and Antonietti has attracted considerable interest owing to its environmental compatibility, cost-effectiveness, earth abundance, thermal and physicochemical stability [18]. Although different kinds of g-C₃N₄ materials with well-defined nanostructures have been developed in the past few years [19–30], intrinsic drawbacks such as marginal visible-light absorption, low surface area and fast electron-hole recombination largely limit their applications in solar-to-fuel conversion.

Recent study has demonstrated that integration of electron-accepting materials on g-C₃N₄ photocatalyst enables faster electron-hole separation and more efficient charge transport, which indirectly boosts hydrogen production performance. So far mainly two kinds of materials, narrow-band semiconductors and carbon-based nanomaterials, were employed as electron acceptors to combine with g-C₃N₄ for the construction of heterostructured photocatalysts for solar-driven water splitting [25,31–41]. The incorporation of other functional materials with moderate conductivity into g-C₃N₄ to fabricate novel composite materials for efficient photocatalytic hydrogen evolution remains largely unexplored. The past decade has witnessed remarkable growth in the controllable synthesis and applications of metal-organic frameworks (MOFs), a family of crystalline porous solids made by linking inorganic and organic units *via* strong coordination bonds. Unique properties including exceptional porosity, structural diversity, high thermal and chemical stability have made MOFs ideal candidates for energy conversion and catalytic applications [42–46]. Zeolitic imidazolate framework-8 (ZIF-8), the most commonly used Zn-containing MOF material, has demonstrated its potentials in the fabrication of functional nanocomposites for a wide variety of applications such as CO₂ absorption and dye photodegradation [47–52], etc.

* Corresponding authors at: School of Materials Science & Engineering, Jiangsu University, Zhenjiang 212013, PR China (X. Yang).
E-mail addresses: xiaofei_yang1980@163.com (X. Yang), tanghua@mail.ujes.edu.cn (H. Tang).

Considering synergistic effects of $g\text{-C}_3\text{N}_4$ semiconductor and ZIF-8, herein we report a two-step strategy to fabricate ZIF-8/modified $g\text{-C}_3\text{N}_4$ composite materials where polyhedral ZIF-8 nanoparticles are uniformly anchored on the surface of rod-like $g\text{-C}_3\text{N}_4$ materials. Electrostatically-driven assembly of ZIF-8 nanoparticles on $g\text{-C}_3\text{N}_4$ rods facilitates the formation of well-organized heterostructures and intimate interfaces. Subsequently the synthesized ZIF-8/ $g\text{-C}_3\text{N}_4$ hybrid materials have been explored for visible-light-responsive photocatalytic hydrogen evolution under white light LED illumination. In principle, this strategy has great potential to be developed as a platform technique for the fabrication of MOF-based composite photocatalytic materials.

2. Experiment section

2.1. Synthesis of modified $g\text{-C}_3\text{N}_4$

Modified $g\text{-C}_3\text{N}_4$ sample was fabricated by mingling a certain mole ratio of trithiocyanuric acid and melamine. Typically, trithiocyanuric acid (10.62 g, 60 mmol) and melamine (7.32 g, 60 mmol) were added into 150 mL deionized water, respectively, followed by an ultrasonic treatment for 10 min. Then trithiocyanuric acid solution was added dropwise into melamine aqueous solution under magnetic stirred for 8 h at room temperature. The precipitate was collected by centrifugation, and washed with deionized water and ethanol repeatedly, dried *in vacuum* at 60 °C for 24 h. The as-prepared yellow powder was transferred into an alumina crucible and calcined at 550 °C in a muffle furnace with a heating rate of 2.3 °C min^{-1} and kept for 4 h. The final yellow products were denoted as CN.

2.2. Synthesis of ZIF-8/modified $g\text{-C}_3\text{N}_4$ composites

The ZIF-8/modified $g\text{-C}_3\text{N}_4$ composites were synthesized by in-situ deposition of ZIF-8 nanoparticles on the above modified $g\text{-C}_3\text{N}_4$ sample CN. In a typical preparation, CN powders with different mass (100 mg, 200 mg, 400 mg, and 800 mg) were dispersed in 150 mL methanol, respectively, followed by an ultrasonic treatment for 8 min. 15 mL zinc nitrate hexahydrate ($\text{Zn}(\text{NO}_3)_2 \cdot 6\text{H}_2\text{O}$, 1.19 g) methanol solution was then added slowly into the corresponding CN suspension with a moderate stirring for 12 h, followed by the addition of 15 mL methanol solution of 2-methylimidazole (Hmim, 2.63 g) into the above mixed solution. When the addition was complete, the mixed solution was aged at room temperature overnight for further hybridization. The obtained precipitates were centrifugated, and washed with deionized water and methanol three times, dried *in vacuum* at 60 °C for 24 h. The final products obtained from different amounts (100 mg, 200 mg, 400 mg, 800 mg) of CN precursor are denoted as ZCN100, ZCN200, ZCN400 and ZCN800, respectively.

2.3. Characterization

The crystal structures and phase composition of the samples were determined by the X-ray diffraction (XRD, D/MAX2500PC), using Cu $K\alpha$ radiation with the 2θ range from 5° to 80° at a scan rate of 5° min^{-1} . The morphological features of the samples were performed by field-emission scanning electron microscopy (FE-SEM, FEI NovaNano450).

The optical property was recorded by UV–vis diffuse reflection spectroscopy (DRS) with a UV2450 spectrophotometer from 200 to 800 nm using BaSO_4 as reference standard. Photoluminescence (PL) emission measurements and transient fluorescence spectra were carried out by a QuantaMaster™ 40 with an excitation wavelength of 395 nm.

2.4. Photocatalytic hydrogen evolution

Photocatalytic H_2 evolution from water splitting experiment was carried out in a gas-closed circulation system with a Pyrex top-irradiation reaction vessel. A 300 W Xe-lamp equipped with a 420 nm cut-off filter was used to provide the visible light irradiation ($\lambda > 420$ nm). In a typical photocatalytic reaction, 10 mg of the as-prepared photocatalyst was dispersed in a 100 mL triethanolamine aqueous solution (10 vol%), which acted as sacrificial reagents, followed by addition of 3 wt% of cocatalyst Pt, which was photodeposited on the photocatalysts. The reaction cell was kept at room temperature with cooling water. Before light irradiation, the system was under vacuum state and prevented from contact with air. The amount of evolved H_2 during light illumination was determined with a gas chromatography equipped with a thermal conductivity detector.

3. Results and discussion

The modification of rod-like $g\text{-C}_3\text{N}_4$ samples was achieved by the self-assembly process and thermal treatment process. In the first step, two symmetric precursors, trithiocyanuric acid (TC) and melamine (M) are able to assemble into supermolecular hydrogen-bonded intermediates with well-organized nanostructures, subsequent calcination of as-prepared well-organized TCM complexes results in the transformation of interconnected polymeric nanostructures into porous $g\text{-C}_3\text{N}_4$. The formation process from porous rod-like (CN) to Zn^{2+} /CN intermediates and final ZIF-8/CN (ZCN) composites is illustrated in Fig. 1. Under ultrasonication, rod-like $g\text{-C}_3\text{N}_4$ materials could be dispersed, the zeta potential of modified rod-like $g\text{-C}_3\text{N}_4$ is determined to be -48 mV. When the precursor $\text{Zn}(\text{NO}_3)_2 \cdot 6\text{H}_2\text{O}$ was added into the $g\text{-C}_3\text{N}_4$ dispersion, positively-charged Zn^{2+} is readily to be absorbed on the surface of negatively-charged $g\text{-C}_3\text{N}_4$ nanorods by electrostatically-driven assembly, the introduction of 2-methylimidazole into the intermediates leads to in situ formation and growth of polyhedral ZIF-8 nanoparticles on porous CN rods, suggesting the generation of ZIF-8/ $g\text{-C}_3\text{N}_4$ (ZCN) composites with controllable interfacial contact.

The morphological features of as-prepared ZIF-8, $g\text{-C}_3\text{N}_4$ materials and the corresponding ZIF-8/ $g\text{-C}_3\text{N}_4$ (ZCN) nanocomposites were evaluated by field-emission scanning electron microscopy (FE-SEM). It is shown in Fig. 2a that ZIF-8 nanoparticles exhibited a highly crystalline polyhedral structure with an average size of 200 nm, while the obtained modified $g\text{-C}_3\text{N}_4$ materials showed rod-like structures where irregular pores are observed on the surfaces (Fig. 2f). When 100 mg $g\text{-C}_3\text{N}_4$ was employed, ZIF-8 nanoparticles are found to be uniformly distributed and deposited on the surface of $g\text{-C}_3\text{N}_4$ rods (Fig. 2b). The addition of 200 mg $g\text{-C}_3\text{N}_4$ materials lead to uneven distribution of ZIF-8 nanoparticles in the ZCN-200 composite, in which the majority of $g\text{-C}_3\text{N}_4$ rods are covered by ZIF-8 nanoparticles and the minority of rods are decorated with scattered ZIF nanoparticles (Fig. 2c). When more

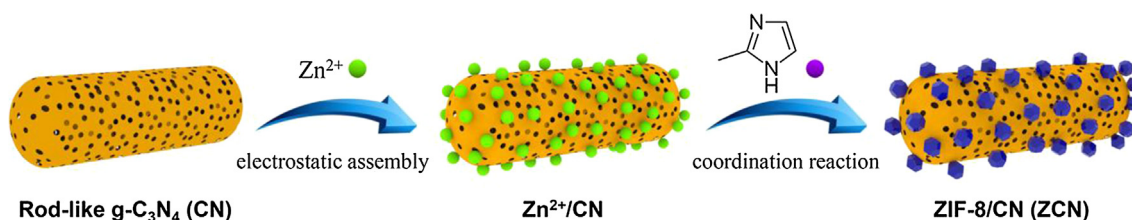


Fig. 1. Schematic diagram of synthesis for ZIF-8/modified rod-like $g\text{-C}_3\text{N}_4$ composites.

Download English Version:

<https://daneshyari.com/en/article/7833176>

Download Persian Version:

<https://daneshyari.com/article/7833176>

[Daneshyari.com](https://daneshyari.com)